Title
Protein engineering to develop a redox insensitive endothelial nitric oxide synthase

Journal
Redox Biology, 2(1)

ISSN
2213-2317

Authors
Rafikov, Ruslan
Kumar, Sanjiv
Aggarwal, Saurabh
et al.

Publication Date
2014

DOI
10.1016/j.redox.2013.12.015

Peer reviewed

Redox Biology 2 (2014) 156–164

Contents lists available at ScienceDirect

Redox Biology

journal homepage: www.elsevier.com/locate/redox

Protein engineering to develop a redox insensitive endothelial nitric oxide synthase ☆

Ruslan Rafikov [a], Sanjiv Kumar [a], Saurabh Aggarwal [a], Daniel Pardo [a], Fabio V. Fonseca [a], Jessica Ransom [a], Olga Rafikova [a], Qiumei Chen [b], Matthew L. Springer [c], Stephen M. Black [a,*]

[a] Pulmonary Vascular Disease, Vascular Biology Center, Georgia Regents University, Augusta, GA, USA
[b] The Cardiovascular Research Institute, University of California, San Francisco, San Francisco, CA, USA
[c] The Division of Cardiology, University of California, San Francisco, San Francisco, CA, USA

ARTICLE INFO

Article history:
Received 18 December 2013
Accepted 19 December 2013
Available online 14 January 2014

Keywords:
Endothelial nitric oxide synthase
Protein engineering
Redox stability
Zinc tetrathiolate cluster

ABSTRACT

The zinc tetrathiolate (ZnS_4) cluster is an important structural feature of endothelial nitric oxide synthase (eNOS). The cluster is located on the dimeric interface and four cysteine residues (C94 and C99 from two adjacent subunits) form a cluster with a Zn ion in the center of a tetrahedral configuration. Due to its high sensitivity to oxidants this cluster is responsible for eNOS dimer destabilization during periods of redox stress. In this work we utilized site directed mutagenesis to replace the redox sensitive cysteine residues in the ZnS_4 cluster with redox stable tetra-arginines. Our data indicate that this C94R/C99R eNOS mutant is active. In addition, this mutant protein is insensitive to dimer disruption and inhibition when challenged with hydrogen peroxide (H_2O_2). Further, the overexpression of the C94R/C99R mutant preserved the angiogenic response in endothelial cells challenged with H_2O_2. The over-expression of the C94R/C99R mutant preserved the ability of endothelial cells to migrate towards vascular endothelial growth factor (VEGF) and preserved the endothelial monolayer in a scratch wound assay. We propose that this dimer stable eNOS mutant could be utilized in the treatment of diseases in which there is eNOS dysfunction due to high levels of oxidative stress.

Introduction

Metallo-enzymes can coordinate zinc ions (Zn) through cysteine or histidine residues. The Zn ion can coordinate four ligands in a tetrahedral structure. In this work we focused on the ZnS_4 cluster in endothelial nitric oxide synthase (eNOS). Endothelial NOS, like all NOS isoforms, is a homodimeric enzyme with the ZnS_4 cluster at the dimeric interface. The cluster is formed by four sulfur atoms from two cysteine residues C94 and C99 from each monomer (Fig. 1). It is well established that the dimeric configuration is required for nitric oxide (NO) generation by NOS [1,2]. Thus, the ZnS_4 cluster is an important contributor to the proper folding of eNOS enzyme. However, the four sulfur atoms in the tetrahedral configuration are very sensitive to oxidation, leading to eNOS dimer disruption and attenuated NO production [3,4]. The distance between sulfur atoms in the ZnS_4 cluster is equal to the distance between sulfur atoms in (S–S) disulfide bond. Therefore, the formation of an intermediate with a two-center three-electron bond between two sulfur atoms is very favorable (Fig. 1) [5]. Further oxidation of the three-electron (S–S) intermediate requires significantly less energy than oxidation of free cysteine, therefore, oxidation of cysteine residues in the ZnS_4 cluster can occur even under conditions of mild oxidative stress.

As eNOS dependent vasodilation is an important mechanism regulating vascular tone, the disruption of eNOS activity under conditions of oxidative stress, can induce pathological changes in blood vessels that can lead to a number of diseases including atherosclerosis, diabetes mellitus and hypertension [6–8]. Thus, maintaining NO production is a primary goal in the treatment of cardiovascular disorders. The purpose of this study was to design an eNOS enzyme that is insensitive to oxidative stress. It has been previously reported that arginine rich structures can be stabilized by the formation of strong electrostatic interactions between arginine residues and negative ions such as phosphate or chloride [9]. We report here that the replacement of the ZnS_4 cluster with a tetra-arginine cluster results in a catalytically competent enzyme.

* Correspondence to: Vascular Biology Center, Georgia Regents University, 1459 Laney Walker Blvd, CB 3211-B, Augusta, GA-30912 USA. Tel.: +1 706 721 7860.
E-mail address: sblack@gru.edu (S.M. Black).

2213-2317/$ - see front matter © 2014 The Authors. Published by Elsevier B.V. All rights reserved.
http://dx.doi.org/10.1016/j.redox.2013.12.015

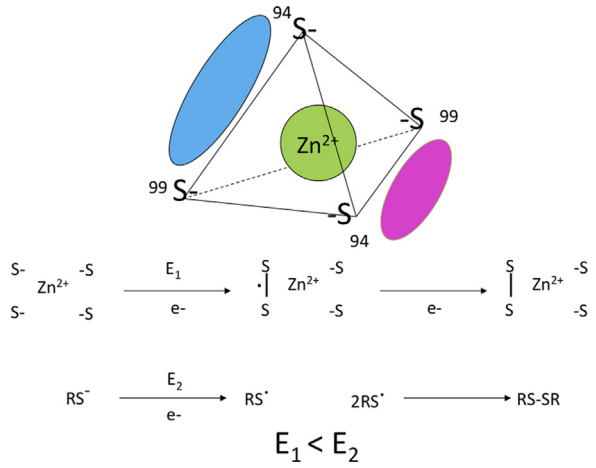

Fig. 1. The structure of Zn-tetrathiolate cluster. The Zn_4 cluster is composed of two cysteine residues (C94 and C99, human nomenclature) from each subunit of eNOS (cyan and magenta). Oxidation of cysteine residues within the Zn_4 cluster requires less energy due to formation of three electron S–S bond in the tetrahedral coordination.

This engineered eNOS is resistant to oxidative dimer disruption and is able to produce NO in an environment of enhanced oxidative stress.

Materials and methods

Molecular dynamic simulations

Molecular dynamic (MD) simulations were performed using Yasara. The Amber 99 all-hydrogen force field was used in the runs (22). For comparison, two 100 nsec simulations at 330 K were carried out using an eNOS dimeric structure. Simulations were carried out within a simulation cube filled with water molecules. All the atoms except those in the 70–125 aa region were fixed. The simulated systems contained ~2000 atoms. Snapshots were saved every 2 ns. Final structures after MD were structurally aligned using the Mustang algorithm in Yasara and the conformational changes were identified.

eNOS protein purification

For eNOS purification, 50 ml of terrific broth was premixed with ampicillin (100 mg/ml) and chlorophenicol (50 mg/ml), and inoculated with E. coli BL21 cells transformed with a polyHis-pCWeNOS plasmid containing wild type human eNOS sequence (9) or the mutant C94R/C99R. The polyHis-pCWeNOS vector was a gift from P. R. Ortiz de Montellano (University of California, San Francisco). The C94R/C99R eNOS mutant was prepared from the wildtype plasmid by Retrogen and sequenced to verify identity. Bacteria were grown overnight at 37 °C (260 rpm) then used to inoculate 2.8 L Fernabach flasks (6 × 1.5 L) again containing terrific broth (52 g/L) as the culture medium and supplemented with ampicillin (100 mg/ml), riboflavin (15 mg), and aminolevulinic acid (0.5 g). Flasks were placed on an orbital shaker and were allowed to grow at 37 °C (200 rpm). The OD_{600} was checked periodically during the growth period until it reached 0.8–1.0 (4–5 h) then adenosine-5′-triphosphate (ATP, 200 μM final concentration) and isopropyl-beta-D-thiogalactopyranoside, dioxane free (IPTG, 1 mM final concentration, to induce the T7 promoter) was added and the cells incubated for 18–20 h at 25 °C (200 rpm). Bacteria were then harvested by centrifugation using a FiberLite F6 6 × 1000 rotor at 4 °C (3500 rpm/2700g) for 20 min. The pellet was immediately transferred into lysis buffer (40 mM Tris–HCl, 5% glycerol, 1 mg/ml lysozyme, 100 mM NaCl, 4 mM FAD, 4 mM FMN, 100 μM BH_4, 5 mM L-arginine) and a protease inhibitor cocktail for use with histidine-tagged proteins (Sigma), ribonuclease A from bovine pancreas (Sigma), and deoxyribonuclease I from bovine pancreas (106 units, Sigma) was added. The pellet was gently rocked for 30 min at 4 °C, sonicated on ice, then subjected to ultracentrifugation at 4 °C (60,000 rpm/37,1000g) for 1 h and 45 min. The supernatant was loaded onto a Hisprep FF 16/10 column (charged with 0.1 M $NiSO_4$) using binding buffer (40 mM Tris–HCl, 100 mM NaCl, 5% glycerol, 30 mM imidazole, 100 μM BH_4, 100 μM L-arginine) at 0.1 ml/min flow. The column was washed with washing buffer (40 mM Tris–HCl, 300 mM NaCl, 5% glycerol, 30 mM imidazole, 100 μM BH_4, 100 μM L-arginine) using a flow rate of 1.5 ml/min, and a base line was obtained resulting in the washing out of non-histidine-tagged proteins. Elution of histidine-tagged protein was accomplished using elution buffer (40 mM Tris–HCl, 300 mM NaCl, 5% glycerol, 400 mM imidazole, 100 μM BH_4, 100 μM L-arginine) at 1.0 ml/min flow. Collected fractions were loaded for size-exclusion gel filtration on a HiLoad 26/60 Superdex 200 prep grade column using eNOS gel filtration buffer (60 mM Tris–HCl, 100 mM NaCl, 5% glycerol, 100 μM BH_4, 100 μM L-arginine) at 0.2 ml/min flow. Fractions were collected in 5 ml amounts for analysis by Coomassie blue staining and Western blot. Desalting was then performed for fractions containing eNOS using a HiPrep 26/10 desalting column and eNOS gel filtration buffer at flow rate of 0.5 ml/min. All purification steps were performed at 4 °C, and the purified protein was stored at −80 °C. Protein homogeneity was confirmed using Coomassie blue staining and Western blot with anti-eNOS antibody with 1:1000 dilutions (Transduction Labs). Final protein concentration was then measured in each fraction.

Gel filtration chromatography

To examine the extent of dimerization in the wildtype and mutant eNOS proteins we utilized analytical gel filtration. One hundred microlitres of each protein, at a concentration of 0.5 mg/ml, was injected into a Tosoh TSKgel G3000SW × l gel filtration column. Using a flow rate of 0.5 ml/min, monomer and dimer fractions were eluted in 100 mM phosphate buffer (pH = 7.0) using an HPLC system (GE) and analyzed by measuring the absorption at 260 nm.

Determination of NO_x levels

To measure NO production we utilized a chemiluminescence method. Wildtype eNOS and the C94R/C99R-eNOS were mixed with the cofactors calmodulin (10 μM) and BH_4 (40 μM) as well as the substrate L-arginine (100 μM) and Ca^{2+} (100 μM $CaCl_2$) in reaction buffer (50 mM HEPES, pH 7.4). The reaction was initiated with the addition of NADPH (10 μM). After 30 min of incubation at 37 °C the reaction mixture was analyzed for NO_x levels. In our experiments, potassium iodide (KI)/acetic acid reagent was prepared fresh daily by dissolving 0.05 g of KI in 7 ml of acetic acid. This reagent was added to a septum sealed purge vessel and bubbled with nitrogen gas. The gas stream was connected via a trap containing 1 N NaOH to a Sievers 280i Nitric Oxide Analyzer (GE). Samples were injected with a syringe through a silicone/Teflon septum. Results were analyzed by measuring the area under curve of the chemiluminescence signal using the Liquid software (GE). To carry out NO measurements in cells experiment, we utilized cell lysate and measured cellular NO content per mg of protein.

Measurement of superoxide levels

To detect superoxide generation, EPR measurements were performed using the spin trap, 1-hydroxy-3-methoxycarbonyl-2,2,5,5-tetramethylpyrrolidine.HCl (CMH) as we have described [10,11].

Optical absorption spectroscopy

The spectra of the wildtype and mutant eNOS proteins were determined using a Shimadzu spectrophotometer using a micro-cuvette. The final protein concentration used was 1 mg/ml. Spectra were scanned at 25 °C in the region 350–600 nm and the average of three measurements was plotted.

Overexpression of eNOS in COS-7 cells and dimer/monomer analysis

COS-7 cells were transfected with wildtype (WT) and C94R/C99R eNOS 48 h before experiment. Cells were treated with increasing concentrations of H_2O_2 (0-, 100-, 200-, 300-, 400-μM). Cells were lysed after the experiment. Lysis buffer containing 1% Triton X-100, 20 mM Tris pH 7.4, 100 mM NaCl, 1 mM EDTA, 1% sodium deoxycholate, 0.1% SDS and protease inhibitor cocktail (Pierce) was then added and insoluble proteins precipitated by centrifugation at 13,000 rpm for 10 min at 4 °C. Samples were mixed with ice cold PBS and ice cold 5 × sample buffer, incubated on ice for 10 min, centrifuged and loaded into 4–20% denaturating polyacrylamide gels (Mini-PROTEAN® TGXTM, BioRad) and low temperature gel electrophoresis (LT-PAGE) was utilized to evaluate the eNOS dimer/monomer ratio. The samples were separated on ice using ice-cold TRIS/Glycine running buffer with 0.1% SDS on 50 V for 3 h. All gels were electrophoretically transferred to PVDF membranes. The membranes were blocked with 1% BSA in Tris-buffered saline (TBS) containing 0.1% Tween 20 for 1 h and incubated overnight at 4 °C with an appropriate dilution of primary antibody anti-eNOS (BD). The membranes were then washed with TBST (3 × 10 min), incubated with secondary antibodies coupled to horseradish peroxidase, washed again with TBST (3 × 10 min), and the protein bands visualized using the Super-Signal West Femto Maximum Sensitivity Substrate (Pierce) on a Kodak 440CF image station. Band intensity was quantified using Kodak 1D image processing software. Protein loading was normalized by reprobing membranes with HSP90 (Sigma).

Endothelial cell culture

Primary cultures of ovine pulmonary arterial endothelial cells (PAEC) were isolated as described previously [12]. Cells were maintained in DMEM containing 1 g/L glucose and supplemented with 10% fetal calf serum (Hyclone, Logan, UT), antibiotics, and antimycotics (MediaTech, Herndon, VA) at 37 °C in a humidified atmosphere with 5% CO_2–95% air. Cells were utilized between passages 3 and 10. COS-7 cells were cultured and maintained in the same constituent medium but with a higher glucose concentration (4.5 g/L glucose).

Scratch wound assay

PAEC were transiently transfected with expression plasmids for either WT- or C94R/C99R-eNOS. The cells were then wounded by scratching the monolayer with a 200 μl pipette tip and washed with medium to remove any debris. Cells were then exposed or not to H_2O_2 (400 μM) and then photographed using phase-contrast microscope (Olympus, Japan) with digital camera 0-, 4-, and 8-h later. The rate of wound healing was determined by measuring the change in distance between the wounded edges over time. The data were plotted as percent change compared to untreated controls.

HMEC-1 migration analysis

An immortalized human microvascular endothelial cell line (HMEC-1) was provided by Dr. Robert Debs and used with permission of its creators, Dr. Edwin Ades and Mr. Francisco J. Candal of the Centers for Disease Control and Dr. Thomas Lawley of Emory University. HMEC-1 cells (passage 8) were seeded in a 6-well plate at 2×10^5 per well and cultured with EBM-2 supplemented with Singlequots (Cambrex) and 5% FBS. 24 h later, 2 μg of DNA (1:1 ratio of WT eNOS with GFP, or C94R/C99R eNOS with GFP) were transfected with PEI solution (gift from R. Debs). After 24 h incubation, GFP+ transfected cells were sorted using a FACS Aria II YG and were cultured for another 24 h before being harvested for migration assays. After detachment, 6×10^3 cells were resuspended in basal cell media (without supplements, 0.5% BSA) and plated in the upper of two chambers divided by a membrane with 8 μm pores (Corning Transwell, Corning, NY). H_2O_2 (Sigma) was added to both the upper and lower chambers at 300 μM. No chemoattractants were used. After 3 h, the membranes were washed twice in PBS and fixed in 4% formaldehyde. After wiping cells off of the upper side of the membrane with a cotton swab (Q-tip), the membranes were detached, dipped briefly in Hoechst 33258 (Invitrogen; 1:2000 in PBS) and mounted on glass slides. Migrated cells were counted on the lower side of the membrane using fluorescence microscopy on 5 random 100 × optical fields per membrane. Each experimental condition was performed in triplicate.

Statistical analysis

Statistical calculations were performed using the GraphPad Prism V. 4.01 software. The mean ± SD or SEM was calculated for all the samples and significance determined using either the unpaired *t*-test or ANOVA. For ANOVA, Newman–Kuels post-hoc testing was also utilized. A value of $P < 0.05$ was considered significant.

Results

Protein engineering of a tetra-arginine cluster based endothelial NOS

We hypothesized that substituting the cysteines that formed ZnS_4 cluster with arginines would still form an active eNOS homodimer, but one that was redox insensitive. Molecular dynamic (MD) experiments were initially undertaken using the available crystal stucture of human eNOS (PDB ID 3NOS) to determine if mutations of the two tetrathiolate clusters generating cysteine residues to arginines (C94R/C99R) would grossly alter the eNOS structure. A phosphate ion (PO_4^{3-}) was introduced as a replacement for the Zn^{2+} ion. The resulting mutant protein was simulated in a water filled cube for 100 ns using the MD simulation module in Yasara. After minimization of free energy, the structure of eNOS was still predicted to be dimeric and three arginine residues were found to interact with the phosphate ion (Fig. 2). Four arginines failed to form a compact tetrahedral structure, however, the structure of catalytic center and substrate channel did not appear to be disturbed in the C94R/C99R mutant eNOS.

Protein purification and characterization of tetra-arginine C94R/C99R eNOS

To begin to analyze the properties of C94R/C99R mutant protein, a histidine tagged protein was expressed and purified using a bacterial expression system and Ni-NTA affinity chromatography. Gel filtration analysis demonstrated that the level of dimer in the purified C94R/C99R eNOS mutant protein was equivalent to that found in WT eNOS (Fig. 3A). This was in contrast to an eNOS mutant in which the ZnS_4 cluster was disrupted by insertion of alanine residues [13] (C94A/C99A, Fig. 3A). Oxidation of the ZnS_4 cluster by H_2O_2 resulted in the disruption of the WT eNOS dimeric structure (Fig. 3B) as previously published [3] while the C94R/C99R mutant eNOS was resistant to H_2O_2-mediated dimer

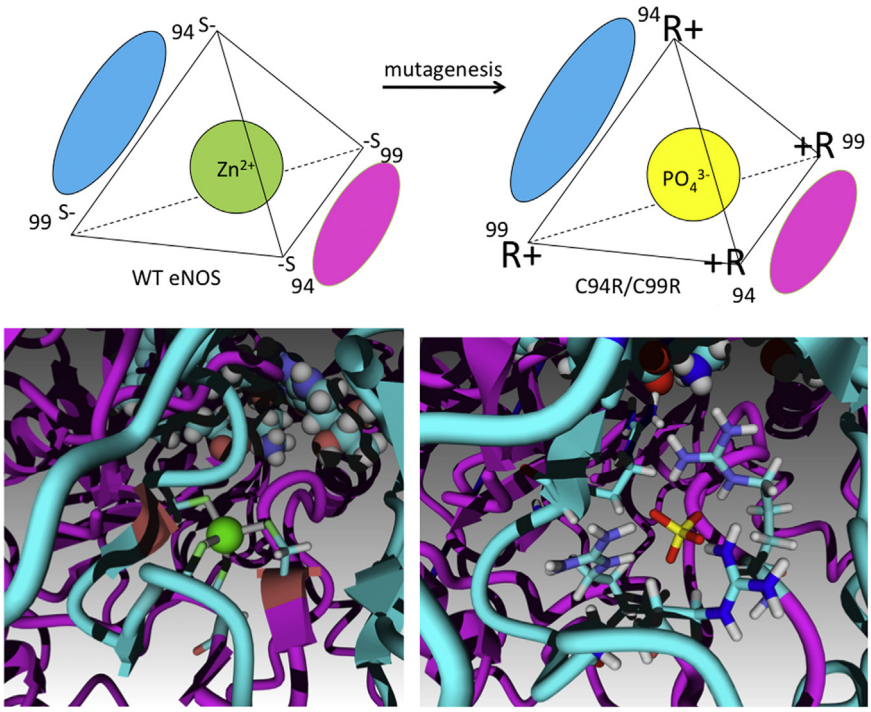

Fig. 2. Ion cluster inversion in C94R/C99R eNOS. The upper panel demonstrates that wildtype eNOS contains a Zn_4 cluster with four negatively charged sulfur atoms surrounding the Zn^{2+} cation in a tetrahedral configuration. In the C94R/C99R mutant the introduction of four arginine residue are proposed to stabilize the dimeric interface of eNOS via electrostatic interactions with a PO_4^{3-} anion. The lower panel shows both the crystal structure of the Zn cluster (PDB ID 3NOS) in wildtype eNOS and computer simulated structure of the C94R/C99R mutant.

disruption (Fig. 3B). Further, we found that H_2O_2 decreased NO generation in WT (Fig. 3C), but not in the C94R/C99R eNOS mutant (Fig. 3D). Interestingly, under basal conditions, the level of NO production was higher in the C94R/C99R mutant compared with that of WT eNOS (Fig. 3C and D). This increase in eNOS activity could be due to the fact that C94R/C99R eNOS mutant is not susceptible to the NO-mediated dimer disruption we have previously shown to occur in WT eNOS. However, further studies will be required to confirm this. Superoxide generation rate of C94R/C99R eNOS was similar to that of wild-type (Fig. 3E). Further we found that the heme spectra in both WT- and C94R/C99R-eNOS have a characteristic band at 396 nm that indicates active high spin heme state (Fig. 3F). Together these data suggest that the inversion of the ion cluster from cation centered ZnS_4 cluster to an anion centered tetra-arginine cluster does not appear to affect the dimeric interface, catalytic and spectral characteristics of the recombinant protein. Moreover, the presence of the tetra-arginine cluster enhances the redox stability of the dimeric eNOS.

Redox stability of C94R/C99R eNOS in COS-7 cells

In order to evaluate the effect of the C94R/C99R mutation on dimeric assembly and susceptibility to oxidative mediated disruption in cells, plasmids encoding WT- and C94R/C99R-eNOS were transiently transfected into COS-7 cells. Our data demonstrated that COS-7 cells expressing the C94/C99R mutant had a higher dimer:monomer ratio than those expressing wildtype eNOS (Fig. 4A and B). Treatment with H_2O_2, which disrupts the ZnS_4 cluster inducing eNOS monomerization [3], led to dose dependant decrease in eNOS dimer levels in WT- but not C94R/C99R-eNOS expressing cells (Fig. 4A and B). Thus, the replacement of redox sensitive tetrathiolate cluster with redox stable four arginines resulted in the stabilization of the enzyme to oxidative stress. We also measured NO generation for both WT- and the C94R/C99R mutant-eNOS. WT- and C999R-eNOS produced similar amount of NO_x under basal conditions (Fig. 4C). H_2O_2 exposure significantly decreased the rate of NO_x generation in WT eNOS expressing cells (Fig. 4C). However, NO_x generation in the C94R/C99R eNOS expressing cells was unaffected by H_2O_2.

C94R/C99R eNOS maintains endothelial cell angiogenesis under conditions of oxidative stress

To determine whether dimer-stable C94R/C99R eNOS protects eNOS-dependent endothelial cell function when exposed to oxidative stress, we transfected ovine PAEC with WT- and C94R/C99R-eNOS and utilized the scratch wound assay. Initially, we confirmed that eNOS protein levels (Fig. 5A) and NO production levels (Fig. 5B) were both increased. Then we assessed the effect on PAEC migration NO production in the presence of H_2O_2. Both NO production (Fig. 5B) and the migration rate (Fig. 5C) were significantly attenuated by H_2O_2 (400 μM) in WT-eNOS expressing cells. However, in PAEC transfected with the redox insensitive C94R/C99R eNOS both NO generation (Fig. 5B) and migration ability were maintained (Fig. 5C).

Finally, we employed a well established, and commonly used, transwell assay for cell migration [14] that has been effective at detecting inhibitory effects on endothelial and endothelial-like cells [15]. HMEC-1 cells, a microvascular endothelial cell line, were transfected with either WT- or C94R/C99A-eNOS and compared to cells transfected with GFP. Our data indicate that under conditions where there were no chemoattractants in the lower chamber, cells both WT- or C94R/C99A-eNOS expressing cells exhibited significantly more random migration than cells transfected with GFP alone (Fig. 5D). However, in the presence of H_2O_2, although migration was decreased in all three groups, there was significantly less reduction in migration in cells transfected with C94R/C99A-eNOS (Fig. 5D).

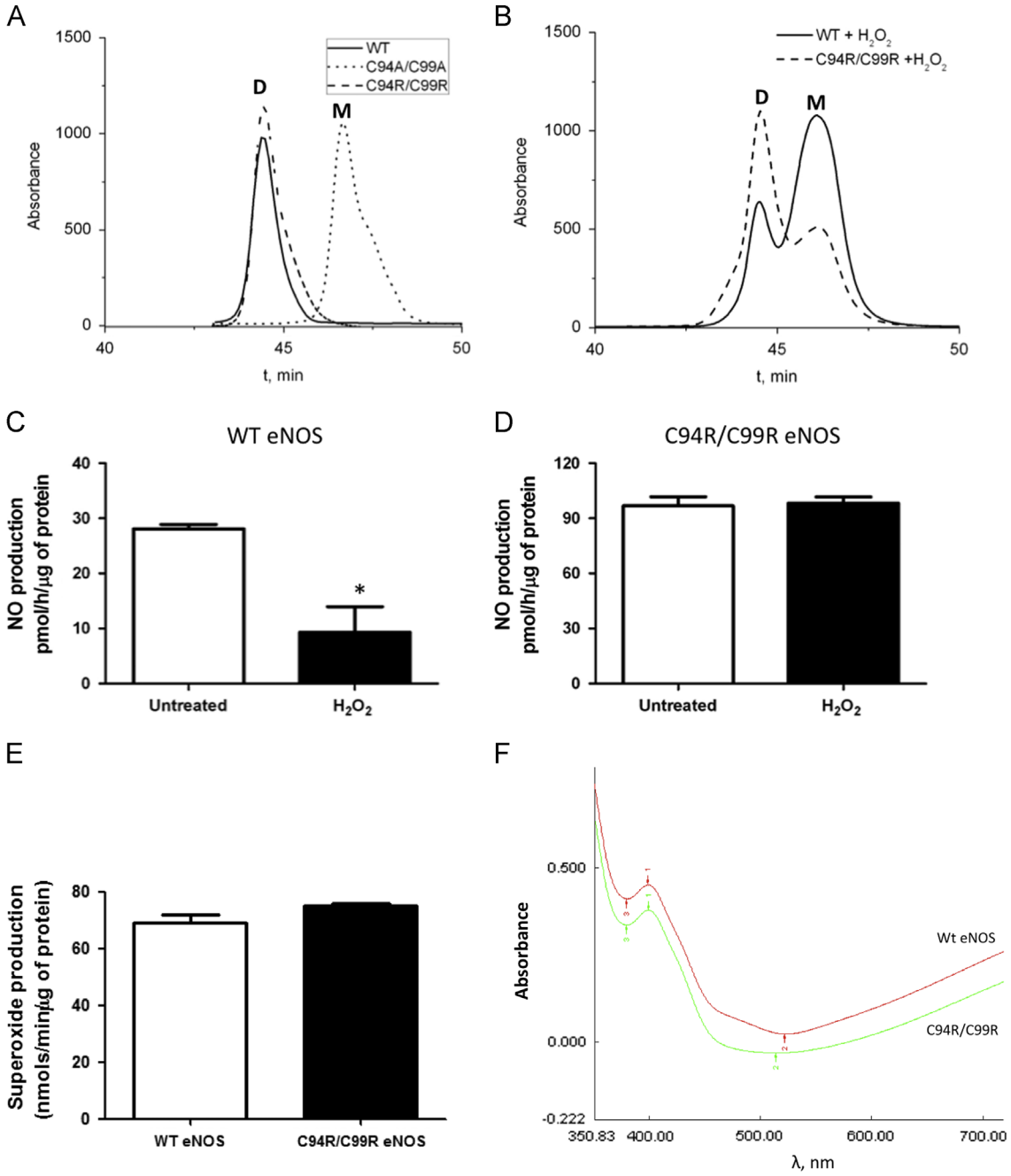

Fig. 3. Characterization of C94R/C99R eNOS mutant. Gel filtration profiles (absorbance at λ260 nm) of WT (solid)-, C94R/C99R (dash)- and C94A/C99A (dot)-eNOS in the presence and absence of H_2O_2 (0.5 mM). WT- and C94R/C99R-eNOS form dimeric proteins in contrast to the C94A/C99A-eNOS mutant (A). H_2O_2 treatment disrupts the dimeric structure of WT eNOS, but the C94R/C99R mutant is resistant to monomerization (B). The disruption of the dimeric structure of WT eNOS correlates with a reduction in NO generation (C). NO generation is maintained in the C94A/C99A-eNOS mutant exposed to H_2O_2 (D). NO production in the C94R/C99R-eNOS under basal conditions is significantly higher that WT-eNOS (C and D) although superoxide generation is similar (E). Both WT- and C94R/C99R-eNOS enzymes exhibited high spin heme absorption peak at 396 nm that indicates catalytically active enzymes. (F). Data are mean ± SEM, N = 3, $^*p < 0.05$ vs. untreated.

Discussion

There is increasing histologic and physiologic evidence that endothelial injury and the resulting aberration in the balance of its regulatory mechanisms play a major role in the development of endothelial dysfunction and vascular remodeling. Endothelial dysfunction is a hallmark of many diseases of the vasculature, including hypertension (both pulmonary and systemic), atherosclerosis, and diabetes [16,17]. The most important consequence of endothelial dysfunction is the observed decrease in the ability of the endothelium to mediate vasodilation [18]. An increasing number of studies now implicate oxidative stress in the pathogenesis of many cardiovascular diseases [19–22]. Oxidative stress is now believed to be a major player in the development of endothelial dysfunction. Further, evidence from both our group and others, has shown a clear correlation between increase in oxidative stress and decrease in both eNOS dimer levels and NO signaling [3,23]. Published data demonstrate that both ROS, such as H_2O_2 [3] and RNS such as NO and peroxynitrite [23–25], can disrupt the eNOS dimer. The mechanism by which this dimer disruption occurs through the oxidation of the ZnS_4 cluster located at the NOS dimer interface was reported previously [3]. Importantly,

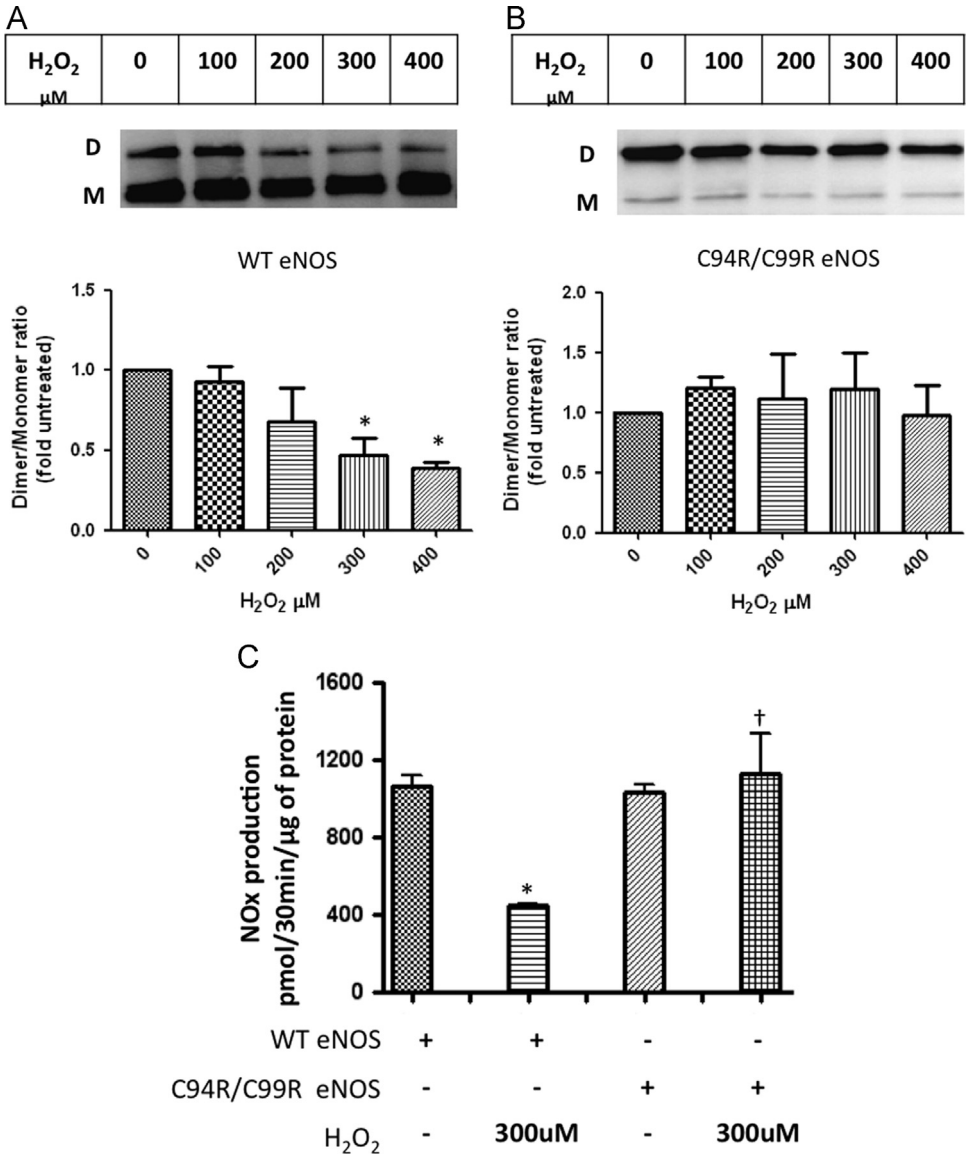

Fig. 4. eNOS dimer stability under conditions of oxidative stress. COS-7 cells were transiently transfected with either WT- or C94R/C99R-eNOS. After 48 h, cells were exposed or not to increasing concentrations of H_2O_2 (0–400 μM, 30 min). Western blot analysis using LT-PAGE, was then used to determine the effect on the eNOS dimer: monomer ratio. H_2O_2 dose dependently decreased the dimer level in WT-eNOS expressing cells (A). However, the C94R/C99R mutant was resistant to dimer disruption even at 400 μM H_2O_2 (B). Basal levels of NO_x were similar in WT- or C94R/C99R-eNOS expressing cells. H_2O_2 exposure (300 μM) significantly reduced NO_x levels in WT eNOS expressing cells but not in the cells expressing the C94R/C99R eNOS mutant (C). Data are mean ± SEM, $N=3$, $^*p<0.05$ vs. untreated; † vs. WT eNOS $+H_2O_2$.

there is a great deal of interest in developing eNOS gene based therapies for the treatment of cardiovascular disease. For example, there is an ongoing clinical trial of a gene therapy for pulmonary hypertension, that is using endothelial progenitor cells, or more accurately, circulating angiogenic cells (CACs) engineered to over-express eNOS [26]. In addition, we, and others have shown that functional deficiencies in CAC migration toward VEGF or association with co-cultured endothelial tubes correlates with endothelial dysfunction and greater risk of cardiovascular events [15,26–31]. Further, CACs have been reported to provide therapeutic benefit when administered directly or i.v. to several models of tissue ischemia or injury [32–35]. The therapeutic effects of CACs can be augmented by transducing them to express vascular regulators, such as VEGF and eNOS [26,36,37]. However, a number of reports have shown that autologous cell therapy can be thwarted if the patient's disease impairs the therapeutic functionality of the cells in question [30,38,39]. In addition, we have demonstrated that CACs isolated from older healthy and CAD donors produce less NO and more ROS than those from young healthy donors and that this is associated not only with impairment of migration toward VEGF, but also with reduced therapeutic capacity when injected into post-MI mouse hearts (MLS, unpublished data). Both negative effects can be improved by transduction of the CACs with an eNOS adenovirus. However, only partial restoration of cardiac function is achieved, even though resistance to NO is not apparent in the impaired CACs [28]. This underscores an important problem in the use of gene based therapies to treat cardiovascular diseases that involve insufficient levels of NO: therapeutic approaches to increase active eNOS protein may nonetheless have limited efficacy due to oxidative-mediated inhibition of the protein through the disruption of the ZnS_4 cluster. Based on these factors, we postulated that there is a potential therapeutic niche for an eNOS protein that was insensitive to oxidative stress mediated dimer disruption and would be able to continue to produce NO under the oxidative stress conditions associated with endothelial dysfunction.

ZnS_4 or zinc histidine–hiolate structural features are found in proteins, such as PKC family enzymes [40], zinc fingers of

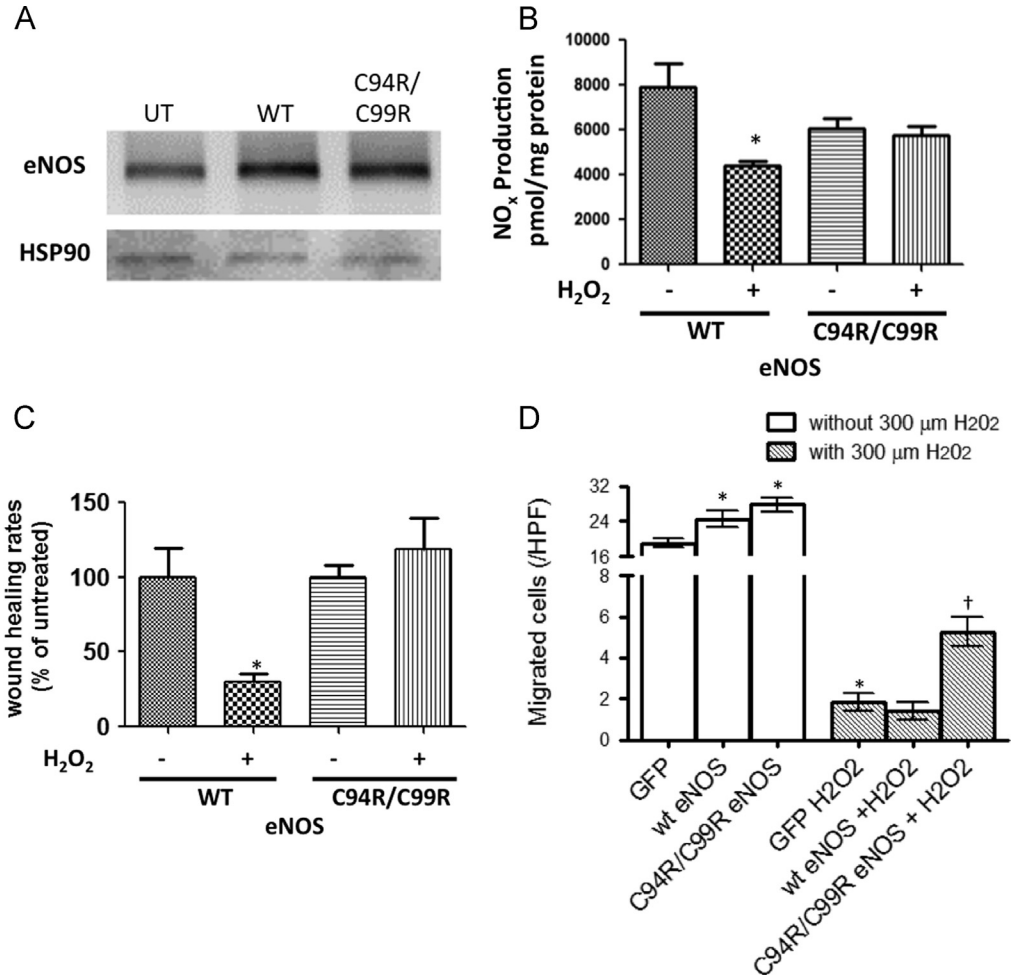

Fig. 5. Effect of eNOS overexpression on endothelial cell migration. PAEC were transiently transfected with either WT- or C94R/C99R-eNOS. After 48 h, eNOS protein levels (A) and basal NO generation were determined. A representative Western blot image is shown that verifies over-expression of both proteins. The blots were reprobed with HSP90 to confirm equal loading. Basal NO_x levels were also significantly increased in WT- and C94R/C99R-eNOS over-expressing cells (B). In the presence of H_2O_2 (400 μM, 1 h), NO_x levels were significantly attenuated in WT- but not C94R/C99R-eNOS over-expressing cells (B). H_2O_2 (400 μM) significantly attenuated wound closure in WT- but not C94R/C99R-eNOS over-expressing cells (C). Similarly, in HMEC-1 cells, cell migration was significantly increased in WT- and C94R/C99R-eNOS over-expressing cells under basal conditions (D). H_2O_2 (300 μM) significantly attenuated HMEC-1 cell migration in both WT- and C94R/C99R-eNOS over-expressing cells (D). However, migration was attenuated less in C94R/C99R-eNOS over-expressing cells (D). Data are mean ± SEM, $N=3$–49, $^*p<0.05$ vs. untreated; $^\dagger p<0.05$ vs. WT-eNOS.

transcription factors [41], sirtuins [42] and metallothionein [43], and NOS [1]. In all cases these form conformational stabilizing structures. In addition, these structural elements share redox sensitivity due to availability of readily oxidazible cysteines [44–46]. However, the presence of a stabilizing tetrathiolate cluster at the dimer interface appears to be an exclusive feature of the NOS isoforms, as a similar structural element has, so far, not been found in other enzymatic systems. Thus, NOS is a unique enzyme that stabilizes its homodimeric structure by employing redox sensitive ZnS_4 cluster. In this work we utilized protein engineering to eliminate this redox sensitivity. There have been several reports utilizing protein engineering to stabilize inter-subunit assembly and, thus, increase the stability of multimeric proteins. These include nucleoside diphosphate kinase [47], acid-sensing ion channel-1a (ASIC1a) [48], and seminal RNAse [49]. The formation of intersubunit bridges also plays an important role in the thermal stability of glucose-6-phosphate dehydrogenase [50]. As with NOS, stabilizing intersubunit disulfide bond formation occurs in many native multimeric proteins. Importantly, for our approach to eNOS, the introduction of an artificial intersubunit disulfide bridge is a well described tactic for the stabilization of a multimeric interface. Indeed, a similar strategy has been utilized to stabilize Fe-superoxide dismutase [51], thymidylate synthase [52] and triosephosphate isomerase [53]. From previous studies we know that there is a disruption of the NOS dimer when the proteins are oxidized by NO, H_2O_2 or peroxynitrite. This involves disulfide oxidation, but does not induce dimer stabilization via disulfides formation in the ZnS_4 cluster. Based on this, we decided to utilize a charge based interactions rather than relying on covalent bonding. In our engineered protein we demonstrate that the replacement of the oxidant sensitive, ZnS_4 cluster with a redox stable, tetra-arginine cluster, produces a fully functional enzyme that is resistant to dimer disruption by oxidative stress and that retains the ability to produce NO under conditions in which the wildtype enzyme is severely inhibited.

It is also worth noting that there is controversy in the literature regarding the relative roles of the ZnS_4 cluster and BH_4, a cofactor essential for the catalytic activity of all three NOS isoforms [54–57], in stabilizing the dimeric interface of NOS [23,24,58–60]. Both are redox sensitive, and the binding site of BH_4 is located in close proximity to the ZnS_4 cluster [1]. Thus, it has been difficult to differentiate the effects mediated by the ZnS_4 cluster from those of BH_4. In addition, prior studies have shown that cellular BH_4 levels have important consequences for the structure of NOS. These include the ability of NOS to shift its heme iron to a high spin state [61], increase arginine binding [61], and at least in some NOS

isoforms, potentially stabilize the active dimeric form of the enzyme [54]. However, based on our published data [3]it is possible that the antioxidant properties of BH_4 is used to protect the ZnS_4 cluster from oxidation during the catalytic cycling of NOS which in turn could explain the apparent dimer stabilizing ability of BH_4. As we show here that the replacement of the ZnS_4 cluster with redox stable tetra-arginines is sufficient to maintain eNOS in a dimeric form under conditions of oxidative stress, we conclude that the ZnS_4 cluster plays the primary role in NOS dimerization.

In conclusion, our engineered C94R/C99R dimer stable mutant opens up the possibility of gene therapy for the treatment of conditions where eNOS dysfunction is associated with increased oxidative stress. This dimer stable enzyme should be able to maintain NO signaling under conditions in which the introduction of the wildtype enzyme would result in dimer disruption and reduced NO generation.

Acknowledgements

This research was supported in part by grants, HL60190 (to SMB), HL67841 (to SMB), HL084739 (to SMB), R21HD057406 (to SMB), HL086917 (to MLS) and P01HL101902 (to SMB) all from the National Institutes of Health, and by a grant from the Foundation Leducq (to SMB). RR and FVF were supported in part by National Institutes of Health Training Grant, 5T32-HL-06699 and OR by F32HL103136. We acknowledge Lejla Medzikovic for technical assistance on this project.

References

[1] C.S. Raman, H. Li, P. Martasek, V. Kral, B.S. Masters, T.L. Poulos, Crystal structure of constitutive endothelial nitric oxide synthase: a paradigm for pterin function involving a novel metal center, Cell 95 (1998) 939–950.
[2] H. Li, C.S. Raman, C.B. Glaser, E. Blasko, T.A. Young, J.F. Parkinson, M. Whitlow, T.L. Poulos, Crystal structures of zinc-free and -bound heme domain of human inducible nitric-oxide synthase. Implications for dimer stability and comparison with endothelial nitric-oxide synthase, J. Biol. Chem. 274 (1999) 21276–21284.
[3] F.V. Fonseca, K. Ravi, D. Wiseman, M. Tummala, C. Harmon, V. Ryzhov, J.R. Fineman, S.M. Black, Mass spectroscopy and molecular modeling predict endothelial nitric oxide synthase dimer collapse by hydrogen peroxide through zinc tetrathiolate metal-binding site disruption, DNA Cell Biol. 29 (2010) 149–160.
[4] M.H. Zou, C. Shi, R.A. Cohen, Oxidation of the zinc-thiolate complex and uncoupling of endothelial nitric oxide synthase by peroxynitrite, J. Clin. Invest. 109 (2002) 817–826.
[5] C. Lu, S. Yao, N. Lin, Studies on reactions of oxidizing sulfur-sulfur three-electron-bond complexes and reducing alpha-amino radicals derived from OH reaction with methionine in aqueous solution, Biochim. Biophys. Acta. 1525 (2001) 89–96.
[6] J.W. Knowles, R.L. Reddick, J.C. Jennette, E.G. Shesely, O. Smithies, N. Maeda, Enhanced atherosclerosis and kidney dysfunction in eNOS(-/-)Apoe(-/-) mice are ameliorated by enalapril treatment, J. Clin. Invest. 105 (2000) 451–458.
[7] S. Cai, J. Khoo, S. Mussa, N.J. Alp, K.M. Channon, Endothelial nitric oxide synthase dysfunction in diabetic mice: importance of tetrahydrobiopterin in eNOS dimerisation, Diabetologia 48 (2005) 1933–1940.
[8] N. Escobales, M.J. Crespo, Oxidative-nitrosative stress in hypertension, Curr. Vasc. Pharmacol. 3 (2005) 231–246.
[9] N.T. Mrabet, A. Van den Broeck, I. Van den brande, P. Stanssens, Y. Laroche, A.M. Lambeir, G. Matthijssens, J. Jenkins, M. Chiadmi, H. van Tilbeurgh, et al., Arginine residues as stabilizing elements in proteins, Biochemistry 31 (1992) 2239–2253.
[10] N. Sud, S. Sharma, D.A. Wiseman, C. Harmon, S. Kumar, R.C. Venema, J.R. Fineman, S.M. Black, Nitric oxide and superoxide generation from endothelial NOS: modulation by HSP90, Am. J. Physiol. 293 (2007) L1444–1453.
[11] P.E. Oishi, D.A. Wiseman, S. Sharma, S. Kumar, Y. Hou, S.A. Datar, A. Azakie, M.J. Johengen, C. Harmon, S. Fratz, J.R. Fineman, S.M. Black, Progressive dysfunction of nitric oxide synthase in a lamb model of chronically increased pulmonary blood flow: a role for oxidative stress, Am. J. Physiol. 295 (2008) L756–766.
[12] S. Wedgwood, S.M. Black, Role of reactive oxygen species in vascular remodeling associated with pulmonary hypertension, Antioxid. Redox Signal. 5 (2003) 759–769.
[13] R. Rafikov, F.V. Fonseca, S. Kumar, D. Pardo, C. Darragh, S. Elms, D. Fulton, S.M. Black, eNOS activation and NO function: structural motifs responsible for the posttranslational control of endothelial nitric oxide synthase activity, J. Endocrinol. 210 (2011) 271–284.
[14] W. Falk, R.H. Goodwin , E.J. Leonard, A 48-well micro chemotaxis assembly for rapid and accurate measurement of leukocyte migration, J. Immunol. Methods 33 (1980) 239–247.
[15] C. Heiss, A. Schanz, N. Amabile, S. Jahn, Q. Chen, M.L. Wong, T. Rassaf, Y. Heinen, M. Cortese-Krott, W. Grossman, Y. Yeghiazarians, M.L. Springer, Nitric oxide synthase expression and functional response to nitric oxide are both important modulators of circulating angiogenic cell response to angiogenic stimuli, Arterioscler. Thromb. Vasc. Biol. 30 (2010) 2212–2218.
[16] K.K. Griendling, D. Sorescu, M. Ushio-Fukai, NAD(P)H oxidase: role in cardiovascular biology and disease, Circ. Res. 86 (2000) 494–501.
[17] K.K. Griendling, D. Sorescu, B. Lassegue, M. Ushio-Fukai, Modulation of protein kinase activity and gene expression by reactive oxygen species and their role in vascular physiology and pathophysiology, Arterioscler. Thromb. Vascular Biol. 20 (2000) 2175–2183.
[18] P.M. Vanhoutte, C.M. Boulanger, Endothelium-dependent responses in hypertension, Hypertens. Res. 18 (1995) 87–98.
[19] N. Anatoliotakis, S. Deftereos, G. Bouras, G. Giannopoulos, D. Tsounis, C. Angelidis, A. Kaoukis, C. Stefanadis, Myeloperoxidase: expressing inflammation and oxidative stress in cardiovascular disease, Curr. Top Med. Chem. 13 (2013) 115–138.
[20] C. Vassalle, S. Bianchi, F. Bianchi, P. Landi, D. Battaglia, C. Carpeggiani, Oxidative stress as a predictor of cardiovascular events in coronary artery disease patients, Clin. Chem. Lab. Med. 50 (2012) 1463–1468.
[21] V. Selvaraju, M. Joshi, S. Suresh, J.A. Sanchez, N. Maulik, G. Maulik, Diabetes, oxidative stress, molecular mechanism, and cardiovascular disease—an overview, Toxicol. Mech. Methods 22 (2012) 330–335.
[22] N.A. Strobel, R.G. Fassett, S.A. Marsh, J.S. Coombes, Oxidative stress biomarkers as predictors of cardiovascular disease, Int. J. Cardiol. 147 (2011) 191–201.
[23] W. Chen, L.J. Druhan, C.A. Chen, C. Hemann, Y.R. Chen, V. Berka, A.L. Tsai, J.L. Zweier, Peroxynitrite induces destruction of the tetrahydrobiopterin and heme in endothelial nitric oxide synthase: transition from reversible to irreversible enzyme inhibition, Biochemistry 49 (2010) 3129–3137.
[24] K. Ravi, L.A. Brennan, S. Levic, P.A. Ross, S.M. Black, S-nitrosylation of endothelial nitric oxide synthase is associated with monomerization and decreased enzyme activity, Proc. Natl. Acad. Sci. USA 101 (2004) 2619–2624.
[25] J. Molnar, S. Yu, N. Mzhavia, C. Pau, I. Chereshnev, H.M. Dansky, Diabetes induces endothelial dysfunction but does not increase neointimal formation in high-fat diet fed C57BL/6J mice, Circ. Res. 96 (2005) 1178–1184.
[26] M.R. Ward, K.A. Thompson, K. Isaac, J. Vecchiarelli, Q. Zhang, D.J. Stewart, M.J. Kutryk, Nitric oxide synthase gene transfer restores activity of circulating angiogenic cells from patients with coronary artery disease, Mol. Ther. 19 (2011) 1323–1330.
[27] C. Heiss, M.L. Wong, V.I. Block, D. Lao, W.M. Real, Y. Yeghiazarians, R.J. Lee, M.L. Springer, Pleiotrophin induces nitric oxide dependent migration of endothelial progenitor cells, J. Cell Physiol. 215 (2008) 366–373.
[28] C. Heiss, S. Jahn, M. Taylor, W.M. Real, F.S. Angeli, M.L. Wong, N. Amabile, M. Prasad, T. Rassaf, J.I. Ottaviani, S. Mihardja, C.L. Keen, M.L. Springer, A. Boyle, W. Grossman, S.A. Glantz, H. Schroeter, Y. Yeghiazarians, Improvement of endothelial function with dietary flavanols is associated with mobilization of circulating angiogenic cells in patients with coronary artery disease, J. Am. Coll Cardiol. 56 (2010) 218–224.
[29] K. Aschbacher, Q. Chen, M. Varga, D.J. Haddad, Y. Yeghiazarians, E. Epel, O. M. Wolkowitz, M.L. Springer, Higher fasting glucose levels are associated with reduced circulating angiogenic cell migratory capacity among healthy individuals, Am. J. Cardiovasc. Dis. 2 (2012) 12–19.
[30] M. Vasa, S. Fichtlscherer, A. Aicher, K. Adler, C. Urbich, H. Martin, A.M. Zeiher, S. Dimmeler, Number and migratory activity of circulating endothelial progenitor cells inversely correlate with risk factors for coronary artery disease, Circ. Res. 89 (2001) E1–7.
[31] C. Heiss, S. Keymel, U. Niesler, J. Ziemann, M. Kelm, C. Kalka, Impaired progenitor cell activity in age-related endothelial dysfunction, J. Am. Coll. Cardiol. 45 (2005) 1441–1448.
[32] C. Kalka, H. Tehrani, B. Laudenberg, P.R. Vale, J.M. Isner, T. Asahara, J.F. Symes, VEGF gene transfer mobilizes endothelial progenitor cells in patients with inoperable coronary disease, Ann. Thorac. Surg. 70 (2000) 829–834.
[33] A. Kawamoto, H.C. Gwon, H. Iwaguro, J.I. Yamaguchi, S. Uchida, H. Masuda, M. Silver, H. Ma, M. Kearney, J.M. Isner, T. Asahara, Therapeutic potential of ex vivo expanded endothelial progenitor cells for myocardial ischemia, Circulation 103 (2001) 634–637.
[34] A.A. Kocher, M.D. Schuster, M.J. Szabolcs, S. Takuma, D. Burkhoff, J. Wang, S. Homma, N.M. Edwards, S. Itescu, Neovascularization of ischemic myocardium by human bone-marrow-derived angioblasts prevents cardiomyocyte apoptosis, reduces remodeling and improves cardiac function, Nat. Med. 7 (2001) 430–436.
[35] V. Schachinger, B. Assmus, M.B. Britten, J. Honold, R. Lehmann, C. Teupe, N.D. Abolmaali, T.J. Vogl, W.K. Hofmann, H. Martin, S. Dimmeler, A.M. Zeiher, Transplantation of progenitor cells and regeneration enhancement in acute myocardial infarction: final one-year results of the TOPCARE-AMI Trial, J. Am. Coll. Cardiol. 44 (2004) 1690–1699.
[36] Y.G. Kong, Z.Y. Ren, C.B. Su, R.Z. Wang, B. Xing, [Expressive level of vascular endothelial growth factor in peripheral blood in patients with pituitary adenomas], Zhongguo Yi Xue Ke Xue Yuan Xue Bao 26 (2004) 164–167.

[37] Y.D. Zhao, D.W. Courtman, Y. Deng, L. Kugathasan, Q. Zhang, D.J. Stewart, Rescue of monocrotaline-induced pulmonary arterial hypertension using bone marrow-derived endothelial-like progenitor cells: efficacy of combined cell and eNOS gene therapy in established disease, Circ. Res. 96 (2005) 442–450.
[38] F.M. Rauscher, P.J. Goldschmidt-Clermont, B.H. Davis, T. Wang, D. Gregg, P. Ramaswami, A.M. Pippen, B.H. Annex, C. Dong, D.A. Taylor, Aging, progenitor cell exhaustion, and atherosclerosis, Circulation 108 (2003) 457–463.
[39] C. Heeschen, R. Lehmann, J. Honold, B. Assmus, A. Aicher, D.H. Walter, H. Martin, A.M. Zeiher, S. Dimmeler, Profoundly reduced neovascularization capacity of bone marrow mononuclear cells derived from patients with chronic ischemic heart disease, Circulation 109 (2004) 1615–1622.
[40] L.T. Knapp, E. Klann, Superoxide-induced stimulation of protein kinase C via thiol modification and modulation of zinc content, J. Biol. Chem. 275 (2000) 24136–24145.
[41] B.L. Vallee, J.E. Coleman, D.S. Auld, Zinc fingers, zinc clusters, and zinc twists in DNA-binding protein domains, Proc. Natl. Acad. Sci. USA 88 (1991) 999–1003.
[42] S.P. Chakrabarty, H. Balaram, Reversible binding of zinc in Plasmodium falciparum Sir2: structure and activity of the apoenzyme, Biochim. Biophys. Acta. 1804 (2010) 1743–1750.
[43] W.F. Furey, A.H. Robbins, L.L. Clancy, D.R. Winge, B.C. Wang, C.D. Stout, Crystal structure of Cd,Zn metallothionein, Science 231 (1986) 704–710.
[44] M.A. Baldwin, C.C. Benz, Redox control of zinc finger proteins, Methods Enzymol. 353 (2002) 54–69.
[45] N.M. Giles, A.B. Watts, G.I. Giles, F.H. Fry, J.A. Littlechild, C. Jacob, Metal and redox modulation of cysteine protein function, Chem. Biol. 10 (2003) 677–693.
[46] W. Maret, New perspectives of zinc coordination environments in proteins, J. Inorg. Biochem. 111 (2012) 110–116.
[47] F. Boissier, F. Georgescauld, L. Moynie, J.W. Dupuy, C. Sarger, M. Podar, I. Lascu, M.F. Giraud, A. Dautant, An intersubunit disulfide bridge stabilizes the tetrameric nucleoside diphosphate kinase of Aquifex aeolicus, Proteins 80 (2012) 1658–1668.
[48] X.P. Chu, N. Close, J.A. Saugstad, Z.G. Xiong, ASIC1a-specific modulation of acid-sensing ion channels in mouse cortical neurons by redox reagents, J. Neurosci. 26 (2006) 5329–5339.
[49] F. Sica, A. Di Fiore, A. Merlino, L. Mazzarella, Structure and stability of the non-covalent swapped dimer of bovine seminal ribonuclease: an enzyme tailored to evade ribonuclease protein inhibitor, J. Biol. Chem. 279 (2004) 36753–36760.
[50] M.M. Altamirano, G. Mulliert, M. Calcagno, Sulfhydryl groups of glucosamine-6-phosphate isomerase deaminase from Escherichia coli, Arch. Biochem. Biophys 258 (1987) 95–100.
[51] K.A. Bunting, J.B. Cooper, I.J. Tickle, D.B. Young, Engineering of an intersubunit disulfide bridge in the iron-superoxide dismutase of Mycobacterium tuberculosis, Arch. Biochem. Biophys. 397 (2002) 69–76.
[52] R.S. Gokhale, S. Agarwalla, V.S. Francis, D.V. Santi, P. Balaram, Thermal stabilization of thymidylate synthase by engineering two disulfide bridges across the dimer interface, J. Mol. Biol. 235 (1994) 89–94.
[53] M. Samanta, M. Banerjee, M.R. Murthy, H. Balaram, P. Balaram, Probing the role of the fully conserved Cys126 in triosephosphate isomerase by site-specific mutagenesis–distal effects on dimer stability, FEBS J. 278 (2011) 1932–1943.
[54] S. Gross, C. Jones, Y. Hattori, C. Raman, Tetrahydrobiopterin: an essential cofactor of nitric oixde synthase with an elusive role. Nitric oixde biology and pathobiology, Academic Press, San Diego, CA (2000) 167–187.
[55] N.S. Kwon, C.F. Nathan, D.J. Stuehr, Reduced biopterin as a cofactor in the generation of nitrogen oxides by murine macrophages, J. Biol. Chem. 264 (1989) 20496–20501.
[56] B. Mayer, B. Hemmens, Biosynthesis and action of nitric oxide in mammalian cells [erratum appears in Trends Biochem Sci 1998 Feb;23(2):87], Trends Bioch. Sci. 22 (1997) 477481.
[57] M.A. Tayeh, M.A. Marletta, Macrophage oxidation of L-arginine to nitric oxide, nitrite, and nitrate. Tetrahydrobiopterin is required as a cofactor, J. Biol. Chem. 264 (1989) 19654–19658.
[58] M. Tummala, V. Ryzhov, K. Ravi, S.M. Black, Identification of the cysteine nitrosylation sites in human endothelial nitric oxide synthase, DNA Cell Biol. 27 (2008) 25–33.
[59] S. Cai, J. Khoo, K.M. Channon, Augmented BH4 by gene transfer restores nitric oxide synthase function in hyperglycemic human endothelial cells, Cardiovasc. Res. 65 (2005) 823–831.
[60] P.A. Erwin, A.J. Lin, D.E. Golan, T. Michel, Receptor-regulated dynamic S-nitrosylation of endothelial nitric-oxide synthase in vascular endothelial cells, J. Biol. Chem. 280 (2005) 19888–19894.
[61] I. Rodriguez-Crespo, N.C. Gerber, P.R. Ortiz de Montellano, Endothelial nitric-oxide synthase. Expression in Escherichia coli, spectroscopic characterization, and role of tetrahydrobiopterin in dimer formation, J. Biol. Chem. 271 (1996) 11462–11467.